Author Manuscript

Author Manuscript

Author Manuscript

Author Manuscript

HHS Public Access

Author manuscript

Nanomedicine (Lond). Author manuscript; available in PMC 2016 June 09.

Published in final edited form as:

Nanomedicine (Lond). 2015 March ; 10(4): 603–614. doi:10.2217/nnm.14.131.

Potentiation of antimicrobial photodynamic inactivation mediated by a cationic fullerene by added iodide: *in vitro* and *in vivo* studies

Yunsong Zhang[1,2,3], **Tianhong Dai**[2,3], **Min Wang**[4], **Daniela Vecchio**[2,3], **Long Y Chiang**[4], and **Michael R Hamblin**[*,2,3,5]

[1]Department of Burn & Plastic Surgery, Guangzhou Red Cross Hospital, Jinan University, Guangzhou, China

[2]Wellman Center for Photomedicine, Massachusetts General Hospital, Boston, MA, USA

[3]Department of Dermatology, Harvard Medical School, Boston, MA, USA

[4]Department of Chemistry, University of Massachusetts, Lowell, MA, USA

[5]Harvard-MIT Division of Health Sciences & Technology, Cambridge, MA, USA

Abstract

Background—Antimicrobial photodynamic inactivation with fullerenes bearing cationic charges may overcome resistant microbes.

Methods & results—We synthesized C_{60}-fullerene (LC16) bearing decaquaternary chain and deca-tertiary-amino groups that facilitates electron-transfer reactions via the photoexcited fullerene. Addition of the harmless salt, potassium iodide (10 mM) potentiated the ultraviolet A (UVA) or white light-mediated killing of Gram-negative bacteria *Acinetobacter baumannii*, Gram-positive methicillin-resistant *Staphylococcus aureus* and fungal yeast *Candida albicans* by 1–2+ logs. Mouse model infected with bioluminescent *Acinetobacter baumannii* gave increased loss of bioluminescence when iodide (10 mM) was combined with LC16 and UVA/white light.

Conclusion—The mechanism may involve photoinduced electron reduction of $^1(C_{60}>)^*$ or $^3(C_{60}>)^*$ by iodide producing $I\cdot$ or I_2 followed by subsequent intermolecular electron-transfer events of $(C_{60}>)^{-}\cdot$ to produce reactive radicals.

Keywords

antimicrobial photodynamic therapy; bioluminescent bacteria; decacationic fullerene; decatertiary-amine chain; *in vivo* infection model; iodide potentiation

For reprint orders, please contact: reprints@futuremedicine.com

*Author for correspondence: Hamblin@helix.mgh.harvard.edu.

Competing interests disclosure

The authors have no other relevant affiliations or financial involvement with any organization or entity with a financial interest in or financial conflict with the subject matter or materials discussed in the manuscript apart from those disclosed.

Ethical conduct of research

The authors state that they have obtained appropriate institutional review board approval or have followed the principles outlined in the Declaration of Helsinki for all human or animal experimental investigations. In addition, for investigations involving human subjects, informed consent has been obtained from the participants involved.

Author Manuscript Author Manuscript Author Manuscript Author Manuscript

Antimicrobial photodynamic inactivation (aPDI) is an emerging approach to kill multidrug resistant bacteria that is rapidly gaining acceptance in the face of the relentless worldwide rise in antibiotic resistance [1,2]. aPDI relies on the use of a harmless dye or photosensitizer (PS) molecule that only becomes microbicidal when excited with the correct wavelength of light [3]. After photon absorption the PS first goes to the short-lived excited singlet state, which can undergo intersystem crossing to the long lived triplet state. The triplet state can then undergo one of two separate processes, both of which can lead to the generation of reactive oxygen species (ROS) that can kill bacteria and other microbial cells. The type 2 photochemical mechanism involves energy transfer from the PS triplet state to ground state molecular oxygen producing the reactive molecule, singlet oxygen. The type 1 photochemical mechanism involves electron transfer from the PS triplet state to oxygen to produce superoxide anion radical, which can subsequently go on to form hydrogen peroxide (H_2O_2) and hydroxyl radicals that are also highly microbicidal.

Fullerenes (C_{60}, C_{70} and C_{84}) are a class of closed cage carbon molecules with a large number of conjugated double bonds that efficiently absorb light in the UV and visible spectral regions [4]. The excited singlet state undergoes efficient intersystem crossing giving these molecules a high triplet quantum yield. Pristine fullerenes are highly hydrophobic and insoluble in aqueous media making them largely unsuitable for biological applications. However the fullerene carbon cage can be derivatized by attachment of organic ligands containing suitable functional groups to provide water solubility and to enable the fullerenes to recognize and bind to biological targets such as bacterial cells. One of the most suitable functional groups for both these purposes is the quaternary ammonium group that provides constitutive cationic charges [5].

Antimicrobial photodynamic therapy (aPDT) involves the use of an aPDI approach *in vivo* to treat a microbial infection in animals [6] or potentially in humans [7]. The PS is topically applied to the infected tissue under conditions where it selectively binds to the invading microbial cells, but not to the host mammalian cells. After an appropriate incubation time (usually relatively short) to allow the PS to penetrate the bacteria but not the host cells, the infected tissue is illuminated with the correct wavelength of light to excite the PS to produce ROS and kill the bacteria without causing collateral tissue damage. Our laboratory has developed an approach to study aPDT for infections in small-animal models of localized infections using bioluminescent microbial cells and noninvasive real-time low-light optical imaging [8]. This technique has many advantages over the traditional alternative of animal sacrifice, tissue homogenization and counting of colony forming units.

The use of fullerenes as PS to mediate photodynamic inactivation (PDI) and photodynamic therapy (PDT) may be one of the most promising biomedical applications of nanotechnology [4,9,10]. Although their absorption spectrum is mainly in the shorter wavelength regions of the electromagnetic spectrum, fullerenes have several properties that make them advantageous. Fullerene molecules have high photostability that makes them resistant to photobleaching that can be the limiting factor in the case of more usual PS derived from tetrapyrrole or phenothiazinium structures. They are particularly effective at

Author Manuscript Author Manuscript Author Manuscript Author Manuscript

mediating Type 1 photochemical mechanisms as opposed to the Type 2 generation of singlet oxygen that dominates other PS.

Acinetobacter baumannii is a pathogenic Gram-negative bacterial species that has become notorious for both innate and acquired antibiotic resistance, and for causing intractable infections in traumatic wounds and burns as well as pneumonia and other systemic infections. *A. baumannii* has been referred to as 'Iraqibacter' due to its seemingly sudden emergence in military treatment facilities during the Iraq War [11]. This species has a particular ability to survive on artificial surfaces for an extended period of time therefore allowing it to persist in the hospital environment. Its virulence and resistance mechanisms are multifarious and include AbaR-type resistance islands, beta-lactamase expression, possession of a polysaccharide capsule, biofilm formation, multidrug efflux pumps and OmpA-mediated host cell adhesion [12]. Panresistant *A. baumanii* infections may only respond to treatment with polymyxins such as colistin with the consequent risk of kidney damage [13]. Methicillin-resistant *Staphyloccus aureus* (MRSA) is arguably the most troublesome of the resistant pathogens causing annual costs of US$14 billion in the United States [14]. *Candida albicans* is responsible for the majority of invasive fungal infections and drug-resistance (especially to azoles) is also rapidly increasing [15].

We have previously reported that localized infections caused by *A. baumannii* respond well to aPDT. A mouse model of a third degree burn infection infected by bioluminescent *A. baumannii* responded to aPDT mediated by polyethylenimine chlorin (e6) conjugate [16] and also by new methylene blue [17] when excited by the appropriate wavelength of red light. Furthermore a C_{70} fullerene adduct was able to treat a similar mouse *A. baumannii* burn infection when excited by UVA light [18].

In the present study we tested the hypothesis that aPDI/aPDT mediated by a C_{60} fullerene bisadduct could be potentiated by addition of the harmless inorganic salt, potassium iodide. *In vitro* studies with members of three different classes of pathogen were carried out to demonstrate the broad-spectrum nature of the approach. An *in vivo* study with a drug-resistant *A. baumannii* strain originally isolated from a US soldier [16], showed that iodide also potentiated fullerene PDT of infections in living mice.

Materials & methods

Synthesis of LC16

Incorporation of a high number of cationic charges on a fullerenyl monoadduct structure requires the synthesis of a hydrophilic addend containing the same number of cationic moieties. In this study, we used a well-defined water-soluble pentacationic *N,N′,N,N,N,N*-hexapropyl-hexa(aminoethyl)amine arm moiety $C_3N_6^+$ with the number of positive charge being fixed at five per arm using methods similar to those previously described [19]. We then attached two quaternary alkylammonium multisalts $C_3N_6^+$ to a malonate linker moiety forming a doubly-armed malonate ester precursor intermediate $N_6^+C_3$-malonate-$N_6^+C_3$, such as $M(C_3N_6^+C_3)_2$, as a plausible approach to assemble a well-defined decacationic addend. Its precursor $M(C_3N_6C_3)_2$ was synthesized in a yield of 78% by an esterification reaction between malonyl chloride and the corresponding hexamine arm $C_3N_6C_3$-OH in

Author Manuscript Author Manuscript Author Manuscript Author Manuscript

CH_2Cl_2 in the presence of pyridine at ambient temperature for a period of 5 h. The quaternization reaction of $M(C_3N_6C_3)_2$ via the addition of an excess of iodomethane portionwise over a period of 3 days at 45°C to afford deca(methyl quaternary ammonium iodide) salt $M(C_3N_6^+C_3)_2$ was carried out in 92% yield, as shown in Figure 1. The use of multiple short hydrophobic *n*-propyl groups was intended to improve and compensate the large incompatibility of two pentacationic $N_6^+C_3$ side-arms with the hydrophobic fullerene moiety in the subsequent reaction and allow the arm-wrapping around the surface of the C_{60} cage. These alkyl interactions along with in-chain charges should promote the solubility of monoadducts in water. The cyclopropanation of C_{60} with $M(C_3N_6^+C_3)_2$ was carried out in a reaction with CBr_4 and 1.8-diazabicyclo[5.4.0]-undec-7-ene (DBU) under different conditions. We found that a reasonable yield of $C_{60}[>M(C_3N_6^+C_3)2]$-$(I^-)_{10}$ was obtained in 65% (Figure 1; after recovery of unreacted C_{60}) with a solvent polarity-balanced mixture of toluene–dimethylformamide (DMF). Subsequent attachment of a second decatertiary-amine malonate arm $M(C_3N_6C_3)_2$ leading to the product of [60]fullerenyl malonate deca(quaternary ammonium iodide) salt $C_{60}[>M(C_3N_6^+C_3)_2][>M(C_3N_6C_3)_2]$-$(I^-)_{10}$ (LC16) was performed by taking a solution of $C_{60}[>M(C_3N_6^+C_3)_2]$ in anhydrous DMF with slow addition of $M(C_3N_6C_3)_2$, CBr_4 and DBU portionwise over a period of 10 h. A chromatographic alumina thin-layered plate with the eluent of ethyl acetate–hexane (4:1, v/v) was used to follow the consumption of $M(C_3N_6C_3)_2$ until its disappearance. After workup and purification, the crude LC16 was obtained in 73% yield and subsequently re-enriched with iodide anions by an ion-exchange reaction with an excess quantity of NaI to recover their lose to bromide ions during the second cyclopropanation reaction. The detailed structural characterization of $C_{60}[>M(C_3N_6^+C_3)_2]$ and LC16 is provided in the Supplementary Material (see online at: www.futuremedicine.com/doi/full/10.2217/NNM.14.131).

Light sources

UVA light (360+/−20 nm; American Ultraviolet Co, IN, USA) was delivered in a spot diameter 15-cm at an irradiance of 20 mW/cm^2. The irradiance was measured using a model IL-1700 research radiometer/photometer (International Light, Inc., MA, USA) using a wavelength range of 250–400 nm. White light source at 400–700 nm (Lumacare, CA, USA) was used to deliver light over a spot diameter 3-cm at an irradiance of 100 mW/cm^2 as measured with a power meter (model DMM 199 with 201 standard head; Coherent, CA, USA).

Bacterial strain & culture conditions

The *A. baumannii* strain that we used in the study was a multidrug-resistant clinical isolate from an injured US soldier deployed to Iraq. It had previously been engineered to be bioluminescent using the lux ABCDE plasmid [16]. The MRSA strain we used was USA300 LAC (Los Angeles County clone), a CA-MRSA strain. The USA300 LAC was chromosomally transduced with the transposon for the bacterial luciferase gene operon lux ABCDE (pAUL-ATn4001 luxABCDE Km(r); Caliper Life Sciences, MA, USA) to give USA300 LAC::lux, allowing a real-time monitoring of the extent of bacterial infection in living [20]. Both bacterial species were routinely grown in brain heart infusion (BHI) medium supplemented with 50 μg/ml kanamycin in an orbital incubator (37°C; 100 rpm)

Author Manuscript Author Manuscript Author Manuscript Author Manuscript

overnight. The overnight suspension was centrifuged, washed with phosphate buffered saline (PBS), and resuspended in fresh BHI medium to a cell density of 10(8) cells/ml (measured by optical density) for experimental use.

The bioluminescent *C. albicans* strain used was CEC 749 as described by a previous study [21]. The luciferase reporter was constructed by fusing a synthetic, codon-optimized version of the Gaussiaprinceps luciferase gene to *C. albicans* PGA59, which encodes a glycosylphosphatidylinositol-linked cell wall protein. Luciferase expressed from this PGA59-gLUC fusion was localized at the *C. albicans* cell surface allowing the detection of luciferase in intact cells after the addition of the luciferase substrate, coelenterazine. *C. albicans* was routinely grown at 30°C on yeast peptone dextrose (YPD) agar and subcultured in YPD medium to an optical density of 0.65 at 570 nm, which corresponds to 10^7 colony-forming units (CFU)/ml. This suspension was then centrifuged, washed with PBS and resuspended in PBS at the same cell density for experimental use.

In vitro PDI studies

3 ml of *A. baumannii* or MRSA suspension both at approximately 10(8) CFU/ml, or 3 ml of *C. albicans* at approximately 10(7) CFU/ml in PBS were incubated with LC16 at a concentration of 20 uM for 20 min. After the incubation time was complete 30 uL of 1M solution of potassium iodide (or PBS as a control) was added to bring the final KI concentration to 10 mM and the suspensions were immediately transferred into a 35-mm petri dish at room temperature (21°C). The suspensions were irradiated with the white light Luma-Care lamp (LumaCare Medical group, CA, USA) at an irradiance of 100 mW/cm^2 or with the UVA lamp at an irradiance of 20 mW/cm^2 with the lid of the petri dish removed. During light irradiation, the suspension was gently stirred by a mini-magnetic bar (Fisher Scientific Co., GA, USA) at 20 rpm. Aliquots of 30 μl of the suspension were withdrawn at 0, 5, 10, 15 and 20 min, respectively, when 0, 30, 60, 90 and 120 J/cm^2 white light or at 0, 4, 8, 12 and 16 min, when 0, 5,10, 15 and 20 J/cm^2 UVA light had been delivered. Light controls received light + KI but no LC16. CFU were then determined by serial dilution on BHI agar (YPD agar for *Candida*) plates by the method of Jett *et al.* [22]. Colonies were allowed to grow for 18–24 h at 37°C for bacteria and at 30°C for *Candida*. The experiments were performed in triplicate.

Bioluminescence imaging

The bioluminescence imaging system (Hamamatsu Photonics KK, NJ, USA) has been previously described [23]. It consisted of an intensified charge-coupled device camera that was mounted in a light-tight specimen chamber and fitted with a light-emitting diode, a setup that allowed a background grayscale image of the entire mouse to be captured. After accumulating binary photon information using an integration time of 2 min, a pseudo-color luminescence image was generated. Using the ARGUS software (Hamamatsu Photonics), the luminescence image was presented as a false-color image superimposed on top of the grayscale reference image. The camera was also connected to a computer system with Microsoft Windows 98 through an image processor (Argus-50, Hamamatsu Photonics). By using Argus-50 control program (Hamamatsu Photonics), the image was acquired and digitally processed to provide pixel intensity over the region of interest.

Author Manuscript Author Manuscript Author Manuscript Author Manuscript

Mouse model of skin-abrasion infected *A. baumannii*

All animal procedures were approved by the Subcommittee on Research Animal Care (IACUC) of Massachusetts General Hospital and met the guidelines of the NIH. Adult female BALB/c mice, 6–8 week old and weighing 17–21 g were used (Charles River Laboratories, MA, USA). The animals were housed one per cage and maintained on a 12-h light/dark cycle, access to food and water ad libitum. At days 4 and 1 before the infection, mice were administered two intraperitoneal injections of cyclophosphamide (the first dose was 150 mg/kg mouse body weight, the second dose was 100 mg/kg). This treatment reduced peripheral blood neutrophils providing a more vulnerable environment in the mice to infection as we have described previously [16]. The mice were anesthetized with *i.p.* injections of ketamine/xylazine cocktail, then were shaved on the dorsal surfaces. Skin abrasion wounds were made on the dorsal surfaces of mice using 28-gauge needles (Micro-Fine IV, Becton Dickinson, NJ, USA) by creating 6 × 6 crossed scratch lines within a defined 1 × 1 cm^2 area. The depth of the wound was no more than the shallow dermis. 5 minutes after wounding, an aliquot of 60 μl suspension containing 10^7 CFU of bioluminescent *A. baumannii* in PBS was inoculated over each defined area containing the scratches with a pipette tip. Bioluminescence images were taken immediately after the inoculation of bacteria to ensure that the bacterial inoculum applied to each abrasion was consistent.

In vivo PDT

Thirty minutes after application of the bacteria to the abrasions, LC16 (200 μM) alone or LC16 (200 μM) + KI (10 mM) solution was added to the PDT-treated wound and also to dark controls. Initially, 40 μL of the PS solution was added to the abrasions and during the light irradiation another addition of 20 μl was added. 10 min after the first addition to allow the PS to bind to and penetrate the bacteria, the mice were again imaged using luminescence camera to quantify any dark toxicity to the bacteria. Mice were then illuminated with UVA at an irradiance of 20 mW/cm^2 or white light at an irradiance of 100 mW/cm^2 as described above. An aluminum foil template was constructed to expose the wound and 1.0 cm of surrounding normal tissue. Mice were given total fluences of up 20 J/cm^2 for UVA light and 120 J/cm^2 for white light in aliquots with luminescence imaging taking place after each aliquot of light.

Statistical methods

Means were calculated and compared for statistical significance using a Student's *t*-test. The time courses of bacterial luminescence imaging were calculated by the use of numerical integration. Differences between all the groups were compared for statistical significance by one-way analysis of variance (ANOVA). p-values of <0.05 were considered significant.

Results

In vitro antibacterial PDI experiments

We initially tested the combination of fullerene PDT + KI for *in vitro* antibacterial PDI in *A. baumannii.* The killing curves are shown for LC16 and LC16 combined with KI are shown

Author Manuscript Author Manuscript Author Manuscript Author Manuscript

in Figure 2. We excited the fullerene with white light and with UVA light as there was some evidence that the photochemical mechanism that followed upon fullerene illumination depended on the excitation wavelength [24]. We delivered increasing fluences of light after incubating the bacteria with a constant concentration of 20 μM fullerene with or without the addition of 10 mM KI. The ratio of fluences of UVA or white light employed was roughly in line with the relative absorption coefficients in the spectrum of LC16. This meant that we delivered up to 20 J/cm^2 of UVA light, and up to 120 J/cm^2 of white light, or sixfold more. Although it is not possible to precisely measure the number of photons absorbed from each light source because of the wide band-widths employed, we feel that a sixfold difference in fluence is reasonable. When LC16 was excited by UVA light (Figure 2A) it killed 1.5 logs of *A. baumanii* at 15 J/cm^2 and 2.5 logs at 20 J/cm^2. UVA light alone (no fullerene) killed less than 1 log even at 20 J/cm^2. When 10 mM KI was added to the incubation mixture the bacterial killing was significantly potentiated with 2.5 logs at 15 J/cm^2 ($p < 0.001$) and 4.5 logs at 20 J/cm^2 ($p < 0.001$). The data with white-light excitation are shown in Figure 2B. There was no significant bacterial killing with white light alone as expected. LC16 at 20 μM excited with white light killed 1.5 logs at 90 J/cm^2 and 1.5 logs at 120 J/cm^2. Addition of 10 mM KI significantly potentiated the killing with 2.5 logs at 90 J/cm^2 ($p < 0.001$) and 4 logs at 120 J/cm^2 ($p < 0.001$). The degree of potentiation by KI appeared to be very similar regardless of whether UVA light or white light was used to excite LC16.

The positive effects of iodide potentiation in the case of Gram-negative *A. baumannii*, encouraged us to test the *Gram-positive* species MRSA. The data are shown in Figure 3.

With UVA there was more than 1 log of potentiation with KI (from 1.8 to 3 logs of killing after 15 J/cm^2; from 2.7 logs to 4.1 logs after 20 J/cm^2). With white-light excitation there was again about 1 log of potentiation with KI at 90 and 120 J/cm^2. These increases were all highly significant ($p < 0.001$).

Finally, to confirm the broad-spectrum nature of this enhancement of PDI killing by addition of KI, we tested the fungal yeast *C. albicans.*

Although the overall killing of *C. albicans* by fullerene-mediated PDI was lower than that found for the bacterial species, we nevertheless were able to demonstrate a significant ($p < 0.001$) potentiation by addition of KI (almost 1 log more killing) with both UVA light (Figure 4A) and with white light (Figure 4B).

In vivo studies in a mouse infection model using bioluminescent *A. baumannii* & *in vivo* imaging

Considering the impressive potentiation of killing obtained by addition of KI in the *in vitro* PDI studies, we tested whether KI could also potentiate the PDT-mediated bacterial killing in an *in vivo* infection model. We monitored the killing of bacteria in the wound by capturing successive bioluminescence images obtained from a mouse abrasion infected with *A. baumannii* and treated with PDT. The infected abrasion was treated with 200 μM of LC16, with and without the addition of 10 mM of KI and excited with UVA light up to 20 J/cm^2 while the control groups were dark controls with the same amount of LC16 + KI and light alone control received UVA light to 20 J/cm^2. The results are shown in Figure 5 where

Author Manuscript Author Manuscript Author Manuscript Author Manuscript

it can be seen that a complete elimination of the bioluminescence signal was observed after a UVA dose of 20 J/cm^2 was delivered in the presence of LC16 + KI. However, the LC16 + UVA group without added KI still had bioluminescence signals remaining in the wound. Both light and dark controls had no measurable diminution in bioluminescence signal during the course of the experiment.

The results of the experiment using white light to excite the fullerene/iodide combination are shown in Figure 6. The loss of bioluminescence signal was slightly less pronounced after excitation with 120 J/cm^2 than it was with 20 J/cm^2 UVA light. Nevertheless the addition of iodide also gave a much better bacterial killing when LC16 was excited by white light.

Figure 7A & B shows the light-dose–response curves of the fraction remaining of the normalized bioluminescence signals calculated from the different mouse groups. When UVA was used for excitation of LC16 + KI, it gave a reduction of over 4-logs while LC16 + UVA alone (no KI) gave a reduction of only 2-log of the bioluminescence relative light units (RLU; $p < 0.001$). No significant reduction was seen for either dark or light control. PDT mediated white light excitation of LC16 + KI induced a reduction of ca. 4-log in RLU, while LC16 alone + white light gave a reduction of only 2-log of the bioluminescence relative light units ($p < 0.001$).

Discussion

We have shown that the addition of the harmless and nontoxic salt (KI) has significantly potentiated the antibacterial effects obtained using both *in vitro* PDI, and also *in vivo* PDT of localized infection mediated by UVA or white light excitation of a cationic fullerene bearing an additional tertiary amine chain.

The mechanism of action of the potentiation of fullerene-mediated PDI by addition of iodide anion is interesting and as yet incompletely understood. There potentially could be as many as three separate mechanisms operating. These are: Iodide anion could undergo a one-electron oxidation by transferring the electron to photoexcited fullerenes, $^1(C_{60}>)^*$ or $^3(C_{60}>)^*$, to form iodide radicals (I·), fullerene radical anions $[(C_{60}>)^{-}\cdot]$ and subsequent reactive radical species which are expected to be bactericidal; a large number of iodide anions could act as an additional source of electrons in potentiating the above type 1 electron transfer photochemical mechanism and generating more bactericidal ROS such as hydroxyl radicals; Iodide anion could be oxidized by photochemical mechanisms of either type 1 or by type 2 (in reaction with $^1O_2$ to produce $O_2^{-}\cdot$, H_2O_2 and HO· sequentially) [25] to form either molecular iodine (I_2 or I_3^- by recombination of 2I· and I^-); these species are known to be bactericidal. Furthermore, the original facile formation of transient $(C_{60}>)^{-}\cdot$ is due to the high electron-accepting capability of $^3(C_{60}>)^*$ cage moiety of LC16. Further transfer of this electron from the fullerenyl radical anion to $^3O_2$ yielding $O_2^{-}\cdot$ can occur in a reversible (forward/reverse reactions) manner [26,27] which is consistent with the mechanism reported for solubilized C_{60}-γ-cyclodextrin in water [28]. The forward reaction when it continuously consumes of $O_2^{-}\cdot$ can produce other type of biological damage-causing ROS, such as H_2O_2 and HO· radicals [29]. In a study by Yamakoshi *et al.* [30], the yield of $O_2^{-}\cdot$ was detectable by EPR-spin-trapping measurements using NADH as the electron-donor. Therefore, our

Author Manuscript Author Manuscript Author Manuscript Author Manuscript

addition of a large number of electron-donating iodide anions (10 mM) should induce increased photoradical generation, which is consistent with the observed cytotoxicity increases shown in Figures 2–4 & 7. Further studies are actively under way in our laboratory to tease apart the relative contributions of each of these mechanisms to the iodide potentiation of the microbicidal effect.

It should be noted that iodide (10 mM) is added to the bacteria/fullerene suspension in the presence of PBS, which contains 150 mM sodium chloride. The activity of the iodide anion in the presence of the much larger concentration of chloride anion underlines that the relative redox potentials are of critical importance (iodide = −0.54 V; chloride = −1.36 V).

Another possibly relevant aspect of this interaction between iodide and fullerene is the ability of iodide to quench the fluorescence of various fluorescent dyes and promote intersystem crossing [31]. However the already very high triplet yield of fullerenes suggests this may not be important in the present case.

It is interesting that the potentiating effect of iodide was observed to about the same extent in the three different classes of microbial cells. The decacationic fullerene was designed to bind and penetrate different classes of microbial cells. It is known that Gram-positive bacteria have permeable cell walls, while fungal cells have a less permeable cell wall structure and Gram-negative bacteria have an impermeable cell wall. However the permeability barrier of Gram-negative bacteria can be overcome by polycationic molecules that disturb the lipopolysaccharide structure by displacing the divalent cations Ca^{2+} and Mg^{2+} [32]. The permeability of microbial cells to iodide anion has not been much studied. Although mammalian cells accumulate iodide via the sodium iodide symporter (highly expressed in the thyroid) [33], only a few rare marine bacterial species have been found to accumulate iodide [34]. At present we believe that the chief site of action of iodide is extracellular, but this remains to be experimentally proved.

Although this is the first time to our knowledge that iodide has been shown to potentiate PDT, iodide has been shown to potentiate other different antimicrobial techniques that rely on generation of ROS. Seymour Klebanoff in 1982 described [35] two different systems, both of which had their antibacterial effects highly potentiated by addition of iodide anion. The first utilized the neutrophil enzyme, MPO in combination with H_2O_2, while the second utilized the Fenton reaction (Fe^{2+} + H_2O_2) a well-known source of hydroxyl radicals. The author concluded that the mechanism of Fenton + iodide potentiation of bacterial killing involved the oxidation of iodide by hydroxyl radicals, while the mechanism of potentiation of killing by MPO/H_2O_2 + Iodide was somewhat different. In 1984 Levitz and Diamond [36] used the same two systems (MPO + Iodide; and Fenton + iodide) to inactivate the conidia of fungal species *Aspergillus fumigatus* and *C. albicans* and found significant potentiation by iodide. In the same year Sugar *et al.* [37] demonstrated the efficacy of the Fenton + iodide system in killing the yeast phase of the pathogenic fungus *Blastomyces dermatitidis.*

Our original hypothesis was that the electron-transfer mechanism would be more pronounced when the fullerene was excited by UVA light than it was when excited by white light [24]. This is evidenced by the fact that six-times more white light was required to

Author Manuscript Author Manuscript Author Manuscript Author Manuscript

achieve equivalent killing as was achieved by UVA light. Although the absorption spectrum is higher in the UVA region than the white region, we believe that shorter wavelength higher energy UVA photons are better at initiating electron transfer than lower energy visible photons. However our hypothesis that this difference would be reflected in a relatively greater degree of potentiation by iodide did not turn out to be the case. The equal degree of potentiation by addition of iodide regardless of which wavelength was used to excite the fullerene may suggest that simple intermolecular electron transfer from iodide to the excited fullerene is not the whole story. Subsequent photoinduced reactive radical formation pathway via fullerenyl transient states may be involved.

There have been several reports about PDI of various drug-resistant microbial cells [38]. The consensus finding of these reports is that multiantibiotic resistant bacteria are equally sensitive to PDI killing as their antibiotic naive counterparts. Furthermore it has not yet proved possible to generate resistant clones of microbial cells even after twenty successive of sub-total killing and regrowth. PDT may therefore be a new clinical approach for superficial infections caused by resistant pathogens such as those in wounds [39], burns, oral cavity [40] and nasal decontamination [41].

One of the chief attractions of using potassium (or sodium) iodide as an adjuvant to potentiate the antimicrobial effect of fullerene-mediated PDI is the lack of toxicity of both iodide and fullerene. Nanotoxicology studies have extensively studied the potential adverse effects of fullerenes in animals and in the environment. The relatively indestructible nature of the C_{60} cage has given rise to the fear that undetected accumulation in animals and the environment could prove disastrous in the future. Although some early reports [42,43] found evidence of oxidative stress and lipid peroxidation in fish exposed to fullerenes, a recent report [44] pointed out errors in these studies and concluded fullerenes were of only low toxicity in these fish. Iodide is considered to be of low toxicity [45] as it is an essential element in human nutrition, has been routinely used in its radioactive form to treat thyroid cancer and is recommended as a prophylactic to prevent thyroid uptake of radioiodine in case of nuclear disaster [46].

Further studies are needed to see how generally applicable may be the use of iodide to potentiate aPDI with a range of different antimicrobial PS (for instance, we have unpublished data that photoinactivation using phenothiazinium dyes such as methylene blue is also strongly potentiated by iodide), and to elucidate the relative contributions of the different putative mechanisms that may be involved.

Conclusion & future perspective

The data has shown that addition of the nontoxic salt KI, can potentiate the PDI-mediated killing of both Gram-positive and Gram-negative bacteria mediated by a decacationic fullerene bearing a decatertiary amine chain, excited both by white and UVA light. This synergistic killing was shown both *in vitro* and *in vivo* using a mouse model of an infected skin abrasion. The encouraging results obtained using a cationic fullerene as an antimicrobial photosensitizer combined with nontoxic potassium iodide both *in vitro* and *in vivo* suggest that further work is justified. The following are possible avenues for

Author Manuscript Author Manuscript Author Manuscript Author Manuscript

understanding the mechanism of action and for improving the effectiveness of fullerene PDT as a therapy for localized infection. Synthesis of new polycationic fullerene derivatives with better capacity for electron transfer-mediated photochemistry and with improved selectivity for microbial cells. Synthesis of fullerene derivatives with light-harvesting antennae to shift the range of activating light that can be absorbed towards red wavelengths, hence increasing light-penetration depth into tissue. In order to understand the mechanism of action of iodide potentiation both at a photochemical and a macroscopic level we will study: increased electron transfer; formation of reactive iodide radicals; and formation of bactericidal molecular iodine. We will determine whether PDT killing of different pathogens such as viruses, fungi and parasites can also be potentiated by addition of iodide. It may be possible to investigate simultaneous delivery of fullerene and iodide by preparation of a nano-drug delivery vehicle consisting of fullerene in lipophilic membrane region and iodide in the hydrophilic core region.

Supplementary Material

Refer to Web version on PubMed Central for supplementary material.

Acknowledgments

Financial disclosure

This research was supported by US NIH grants R01AI050875 and R01CA137108. Yunsong Zhang was supported by the Medical Science Foundation of Guangzhou City (grant 20112121220025).

No writing assistance was utilized in the production of this manuscript.

References

1. Tavares LS, Silva CS, De Souza VC, Da Silva VL, Diniz CG, Santos MO. Strategies and molecular tools to fight antimicrobial resistance: resistome, transcriptome, and antimicrobial peptides. Front Microbiol. 2013; 4:412. [PubMed: 24427156]
2. Tillotson GS, Theriault N. New and alternative approaches to tackling antibiotic resistance. F1000Prime Rep. 2013; 5:51. [PubMed: 24381727]
3. Dai T, Huang YY, Hamblin MR. Photodynamic therapy for localized infections-State of the art. Photodiagnosis Photodyn Ther. 2009; 6(3–4):170–188. [PubMed: 19932449]
4. Mroz P, Tegos GP, Gali H, Wharton T, Sarna T, Hamblin MR. Photodynamic therapy with fullerenes. Photochem Photobiol Sci. 2007; 6(11):1139–1149. [PubMed: 17973044]
5. Tegos GP, Demidova TN, Arcila-Lopez D, et al. Cationic fullerenes are effective and selective antimicrobial photosensitizers. Chem Biol. 2005; 12(10):1127–1135. [PubMed: 16242655]
6. Sharma SK, Dai T, Kharkwal GB, et al. Drug discovery of antimicrobial photosensitizers using animal models. Curr Pharm Des. 2011; 17:1303–1319. [PubMed: 21504410]
7. Kharkwal GB, Sharma SK, Huang YY, Dai T, Hamblin MR. Photodynamic therapy for infections: clinical applications. Lasers Surg Med. 2011; 43(7):755–767. [PubMed: 22057503]
8. Demidova TN, Gad F, Zahra T, Francis KP, Hamblin MR. Monitoring photodynamic therapy of localized infections by bioluminescence imaging of genetically engineered bacteria. J Photochem Photobiol B. 2005; 81:15–25. [PubMed: 16040251]
9. Sharma SK, Chiang LY, Hamblin MR. Photodynamic therapy with fullerenes *in vivo*: reality or a dream? Nanomedicine (Lond). 2011; 6(10):1813–1825. [PubMed: 22122587]
10. Sperandio, FF.; Gupta, A.; Wang, M., et al. Photodynamic Therapy Mediated by Fullerenes and Their Derivatives. American Society of Mechanical Engineers/Momentum Press; NY, USA: 2012.

Author Manuscript Author Manuscript Author Manuscript Author Manuscript

11. Calhoun JH, Murray CK, Manring MM. Multidrug-resistant organisms in military wounds from Iraq and Afghanistan. Clin Orthop Relat Res. 2008; 466(6):1356–1362. [PubMed: 18347888]
12. Bonnin RA, Nordmann P, Poirel L. Screening and deciphering antibiotic resistance in *Acinetobacter baumannii*: a state of the art. Expert Rev Anti Infect Ther. 2013; 11(6):571–583. [PubMed: 23750729]
13. Vila J, Pachon J. Therapeutic options for *Acinetobacter baumannii* infections: an update. Expert Opin Pharmacother. 2012; 13(16):2319–2336. [PubMed: 23035697]
14. Lee BY, Singh A, David MZ, et al. The economic burden of community-associated methicillin-resistant *Staphylococcus aureus* (CA-MRSA). Clin Microbiol Infect. 2013; 19(6):528–536. [PubMed: 22712729]
15. Pfaller MA. Antifungal drug resistance: mechanisms, epidemiology, and consequences for treatment. Am J Med. 2012; 125(1 Suppl):S3–S13. [PubMed: 22196207]
16. Dai T, Tegos GP, Lu Z, et al. Photodynamic therapy for *Acinetobacter baumannii* burn infections in mice. Antimicrob Agents Chemother. 2009; 53(9):3929–3934. [PubMed: 19564369]
17. Ragas X, Dai T, Tegos GP, Agut M, Nonell S, Hamblin MR. Photodynamic inactivation of *Acinetobacter baumannii* using phenothiazinium dyes: *in vitro* and *in vivo* studies. Lasers Surg Med. 2010; 42(5):384–390. [PubMed: 20583252]
18. Huang L, Wang M, Dai T, et al. Antimicrobial photodynamic therapy with decacationic monoadducts and bisadducts of [70]fullerene: *in vitro* and *in vivo* studies. Nanomedicine (Lond). 2013; 9(2):253–266. [PubMed: 23738632]
19. Wang M, Maragani S, Huang L, et al. Synthesis of decacationic [60]fullerene decaiodides giving photoinduced production of superoxide radicals and effective PDT-mediation on antimicrobial photoinactivation. Eur J Med Chem. 2013; 63:170–184. [PubMed: 23474903]
20. Plaut RD, Mocca CP, Prabhakara R, Merkel TJ, Stibitz S. Stably luminescent Staphylococcus aureus clinical strains for use in bioluminescent imaging. PLoS ONE. 2013; 8(3):e59232. [PubMed: 23555002]
21. Enjalbert B, Rachini A, Vediyappan G, et al. A multifunctional, synthetic *Gaussia princeps* luciferase reporter for live imaging of *Candida albicans* infections. Infect Immun. 2009; 77(11): 4847–4858. [PubMed: 19687206]
22. Jett BD, Hatter KL, Huycke MM, Gilmore MS. Simplified agar plate method for quantifying viable bacteria. Biotechniques. 1997; 23(4):648–650. [PubMed: 9343684]
23. Hamblin MR, O'Donnell DA, Murthy N, Contag CH, Hasan T. Rapid control of wound infections by targeted photodynamic therapy monitored by *in vivo* bioluminescence imaging. Photochem Photobiol. 2002; 75(1):51–57. [PubMed: 11837327]
24. Sperandio FF, Sharma SK, Wang M, et al. Photoinduced electron-transfer mechanisms for radical-enhanced photodynamic therapy mediated by water-soluble decacationic C(7)(0) and C(8)(4)O(2) fullerene derivatives. Nanomedicine. 2013; 9(4):570–579. [PubMed: 23117043]
25. Gupta AK, Rohatgi-Mukherjee KK. Solvent effect on photosensitized oxidation of iodide ion by anthracene sulphonates. Photochem Photobiol. 1978; 27:539–543.
26. Bensasson RV, Brettreich M, Frederiksen J, et al. Reactions of e^-_{aq}, CO2•$^-$, HO•, O2•$^-$ and O_2 ($^1\Delta_g$) with a dendro[60] fullerene and $C_{60}[C(COOH)_2]_n$ (n = 2–6). Free Radic Biol Med. 2000; 29(1):26–33. [PubMed: 10962202]
27. Stinchcombe J, Penicand A, Bhyrappa P, Boyd PD, Reed CA. Buckminsterfulleride(1-) salts: synthesis, EPR, and the Jahn-Teller distortion of C60- J Am Chem Soc. 1993; 115:5212–5217.
28. Guldi DM, Huie RE, Neta P, Hungerbühler H, Asmus KD. Excitation of C60, solubilized in water by triton X-100 and gamma-cyclodextrin, and subsequent charge separation via reductive quenching. Chem Phys Lett. 1994; 223:511–516.
29. Texier I, Berberan-Santos MN, Fedorov A, et al. Photophysical and photochemistry of a water-soluble C60 dendrimer; fluorescence quenching by halides and photoinduced oxidation of I- J Phys Chem A. 2001; 105:10278–10285.
30. Yamakoshi Y, Umezawa N, Ryu A, et al. Active oxygen species generated from photoexcited fullerene (C60) as potential medicines: O2−* versus 1O2. J Am Chem Soc. 2003; 125(42):12803–12809. [PubMed: 14558828]

Author Manuscript Author Manuscript Author Manuscript Author Manuscript

31. Chmyrov A, Sanden T, Widengren J. Iodide as a fluorescence quencher and promoter – mechanisms and possible implications. J Phys Chem B. 2010; 114(34):11282–11291. [PubMed: 20695476]
32. Minnock A, Vernon DI, Schofield J, Griffiths J, Parish JH, Brown SB. Mechanism of uptake of a cationic water-soluble pyridinium zinc phthalocyanine across the outer membrane of *Escherichia coli.* Antimicrob Agents Chemother. 2000; 44(3):522–527. [PubMed: 10681312]
33. Filetti S, Bidart JM, Arturi F, Caillou B, Russo D, Schlumberger M. Sodium/iodide symporter: a key transport system in thyroid cancer cell metabolism. Eur J Endocrinol. 1999; 141(5):443–457. [PubMed: 10576759]
34. Amachi S, Mishima Y, Shinoyama H, Muramatsu Y, Fujii T. Active transport and accumulation of iodide by newly isolated marine bacteria. Appl Environ Microbiol. 2005; 71(2):741–745. [PubMed: 15691925]
35. Klebanoff SJ. The iron-H_2O_2-iodide cytotoxic system. J Exp Med. 1982; 156(4):1262–1267. [PubMed: 6296262]
36. Levitz SM, Diamond RD. Killing of *Aspergillus fumigatus* spores and *Candida albicans* yeast phase by the iron-hydrogen peroxide-iodide cytotoxic system: comparison with the myeloperoxidase-hydrogen peroxide-halide system. Infect Immun. 1984; 43(3):1100–1102. [PubMed: 6321349]
37. Sugar AM, Chahal RS, Brummer E, Stevens DA. The iron-hydrogen peroxide-iodide system is fungicidal: activity against the yeast phase of *Blastomyces dermatitidis.* J Leukoc Biol. 1984; 36(4):545–548. [PubMed: 6592286]
38. Vera DM, Haynes MH, Ball AR, et al. Strategies to potentiate antimicrobial photoinactivation by overcoming resistant phenotypes. Photochem Photobiol. 2012; 88(3):499–511. [PubMed: 22242675]
39. Morley S, Griffiths J, Philips G, et al. Phase IIa randomized, placebo-controlled study of antimicrobial photodynamic therapy in bacterially colonized, chronic leg ulcers and diabetic foot ulcers: a new approach to antimicrobial therapy. Br J Dermatol. 2013; 168(3):617–624. [PubMed: 23066973]
40. Sigusch BW, Engelbrecht M, Volpel A, Holletschke A, Pfister W, Schutze J. Full-mouth antimicrobial photodynamic therapy in *Fusobacterium nucleatum*-infected periodontitis patients. J Periodontol. 2010; 81(7):975–981. [PubMed: 20350153]
41. Bryce E, Wong T, Roscoe D, Forrester L, Masri B. A novel immediate pre-operative decolonization strategy reduces surgical site infections. Antimicrob Resistance and Infect Control. 2013; 2(Suppl. 1):010.
42. Zhu S, Oberdorster E, Haasch ML. Toxicity of an engineered nanoparticle (fullerene, C60) in two aquatic species, *Daphnia* and fathead minnow. Mar Environ Res. 2006; 62(Suppl):S5–S9. [PubMed: 16709433]
43. Zhu X, Zhu L, Lang Y, Chen Y. Oxidative stress and growth inhibition in the freshwater fish Carassius auratus induced by chronic exposure to sublethal fullerene aggregates. Environ Toxicol Chem. 2008; 27(9):1979–1985. [PubMed: 19086321]
44. Henry TB, Petersen EJ, Compton RN. Aqueous fullerene aggregates (nC60) generate minimal reactive oxygen species and are of low toxicity in fish: a revision of previous reports. Curr Opin Biotechnol. 2011; 22(4):533–537. [PubMed: 21719272]
45. Sherer TT, Thrall KD, Bull RJ. Comparison of toxicity induced by iodine and iodide in male and female rats. J Toxicol Environ Health. 1991; 32(1):89–101. [PubMed: 1987365]
46. Weiss JF, Landauer MR. History and development of radiation-protective agents. Int J Radiat Biol. 2009; 85(7):539–573. [PubMed: 19557599]

Author Manuscript Author Manuscript Author Manuscript Author Manuscript

Executive summary

- A deca-cationic fullerene functionalized with an additional deca-tertiary amine chain attached was used to carry out *in vitro* photodynamic therapy (PDT) of drug-resistant microbial strains, Gram-negative bacteria *Acinetobacter baumannii*, Gram-positive methicillin-resistant *Staphylococcus aureus* and fungal yeast *Candida albicans*.
- Ultraviolet A light was five-times more effective than white light in mediating bacterial killing.
- Addition of nontoxic potassium iodide to the fullerene increased the light mediated killing by a factor of around 100.
- A mouse model of a partial thickness skin abrasion infected with bioluminescent *A. baumanii* showed that the addition of iodide potentiated the PDT-eradication of the infection *in vivo* as well.
- This is the first time that iodide has been shown to potentiate antimicrobial PDT and has potential clinical relevance.

Author Manuscript Author Manuscript Author Manuscript Author Manuscript

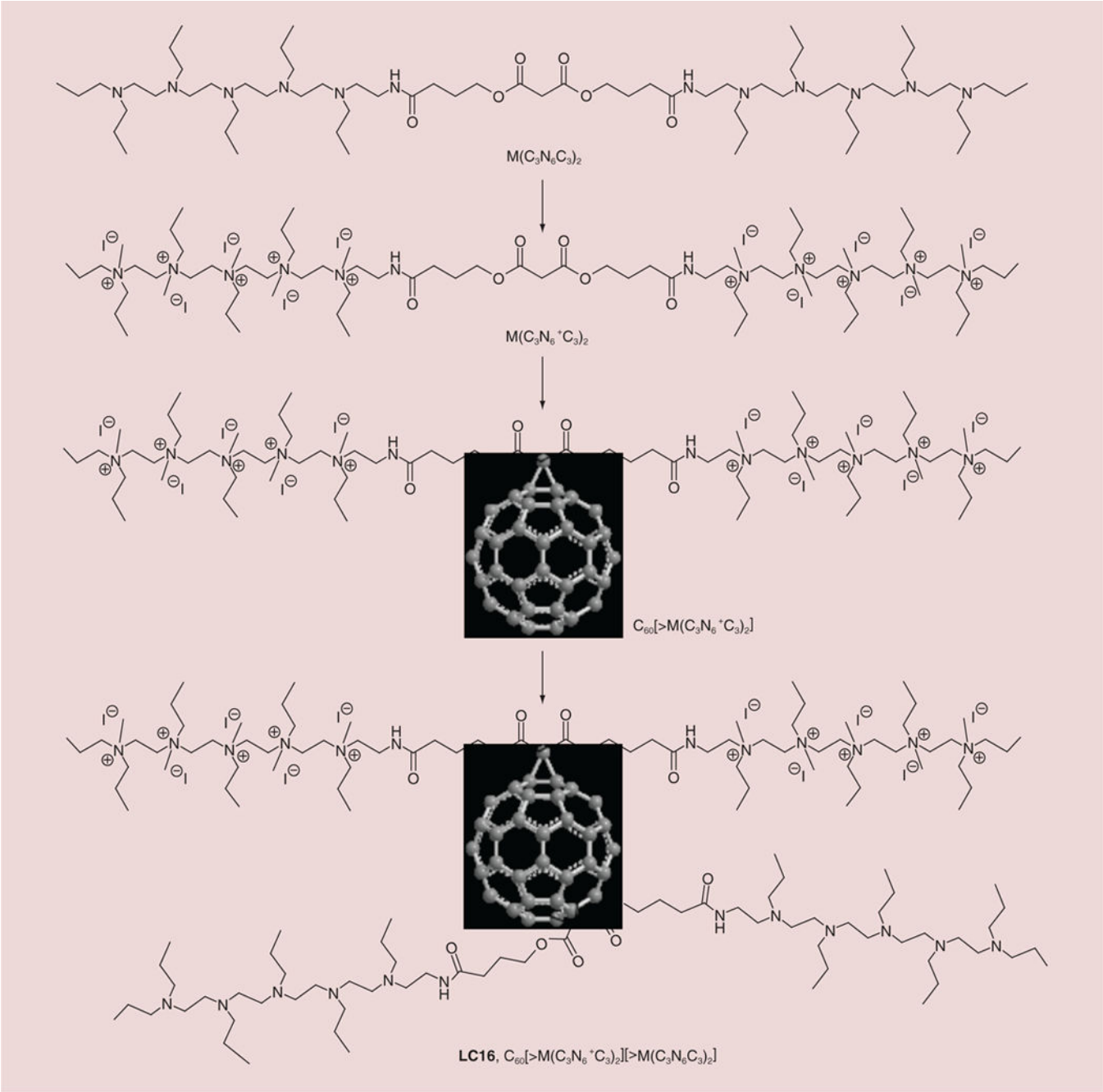

Figure 1. Structure and synthesis of C_{60}-fullerene

LC16: C_{60}-fullerene.

Author Manuscript Author Manuscript Author Manuscript Author Manuscript

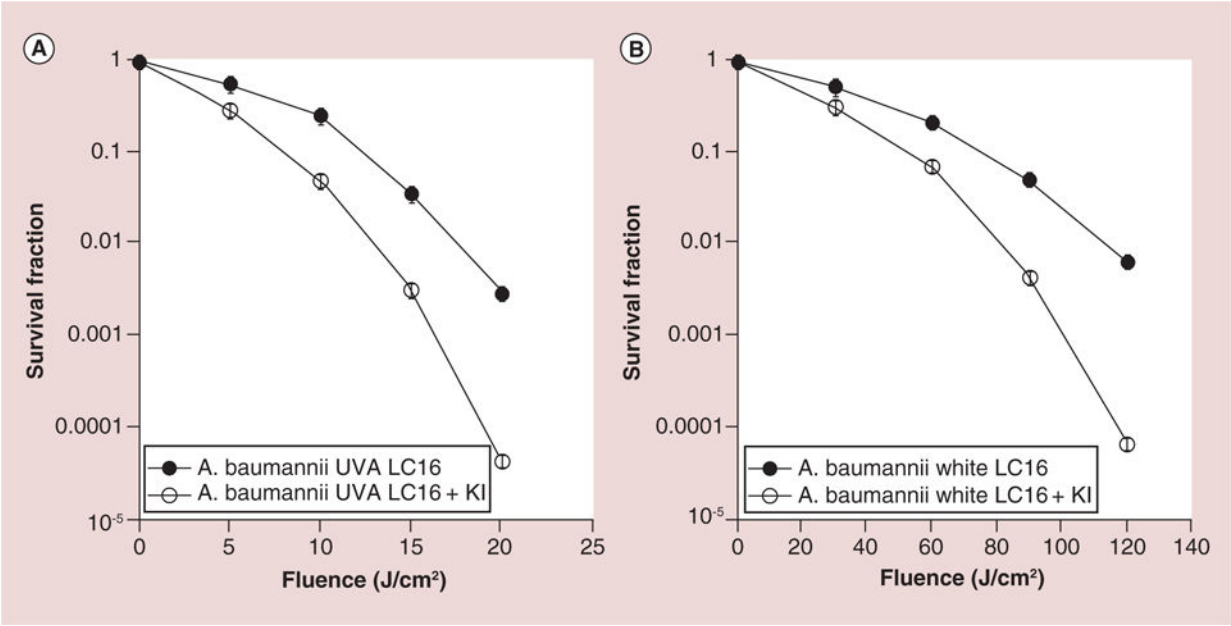

Figure 2. Light dose response for photodynamic inactivation of Gram-negative *Acinetobacter baumannii* mediated by C_{60}-fullerene (20 μM) with and without the addition of KI (10 mM)

(A) UVA light; **(B)** white light. Points are averages of five separate experiments and bars are standard deviations.

LC16: C_{60}-fullerene; UVA: Ultraviolet A.

Author Manuscript Author Manuscript Author Manuscript Author Manuscript

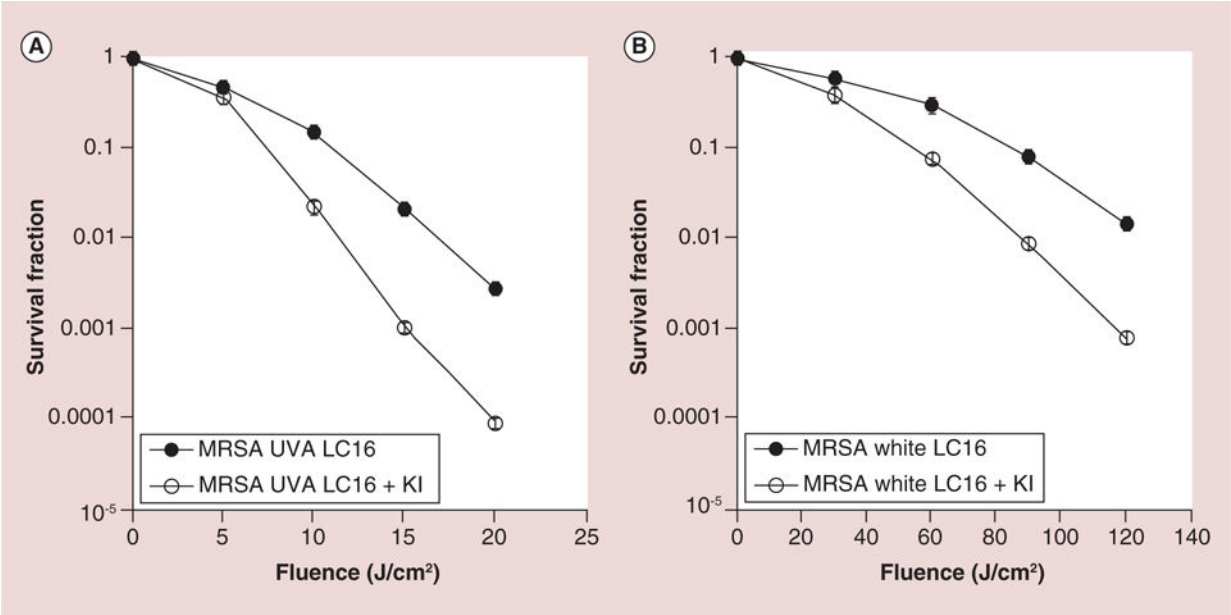

Figure 3. Light dose response for photodynamic inactivation of Gram-positive methicillin-resistant *Staphyloccus aureus* (MRSA) mediated by C_{60}-fullerene (20 μM) with and without the addition of KI (10 mM)

(A) UVA light; **(B)** white light. Points are averages of five separate experiments and bars are standard deviations.

LC16: C_{60}-fullerene; MRSA: Methicillin-resistant *Staphyloccus aureus;* UVA: Ultraviolet A.

Author Manuscript Author Manuscript Author Manuscript Author Manuscript

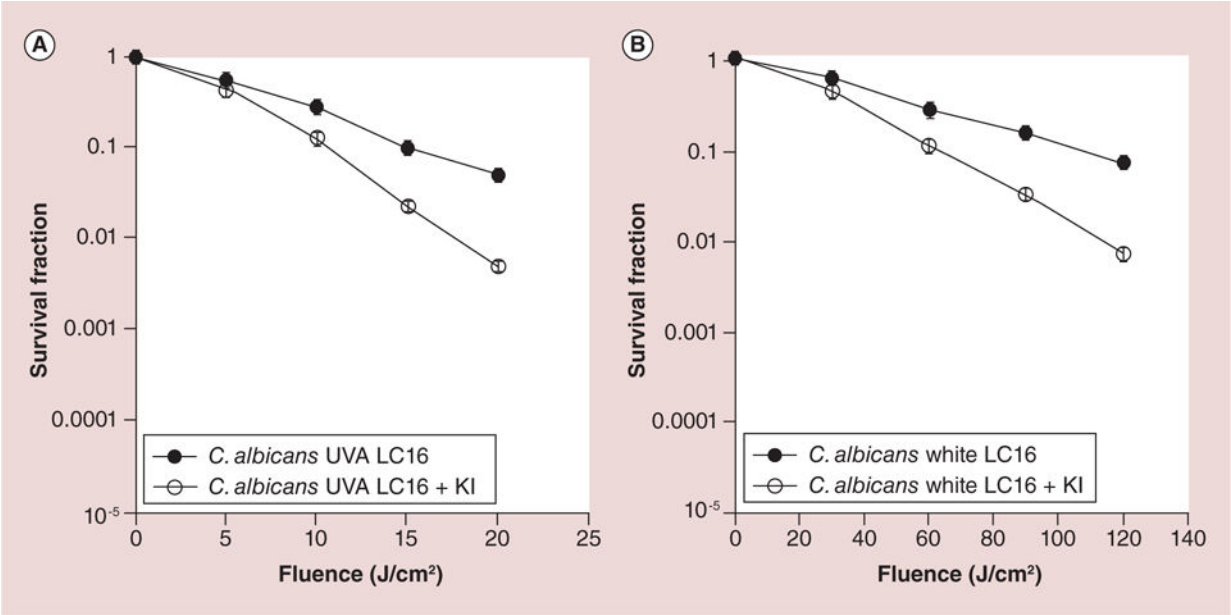

Figure 4. Light dose response for photodynamic inactivation of fungal yeast *Candida albicans* mediated by C_{60}-fullerene (20 μM) with and without the addition of KI (10 mM)

(A) UVA light; **(B)** white light. Points are averages of 5 separate experiments and bars are standard deviations.

LC16: C_{60}-fullerene; UVA: Ultraviolet A.

Author Manuscript Author Manuscript Author Manuscript Author Manuscript

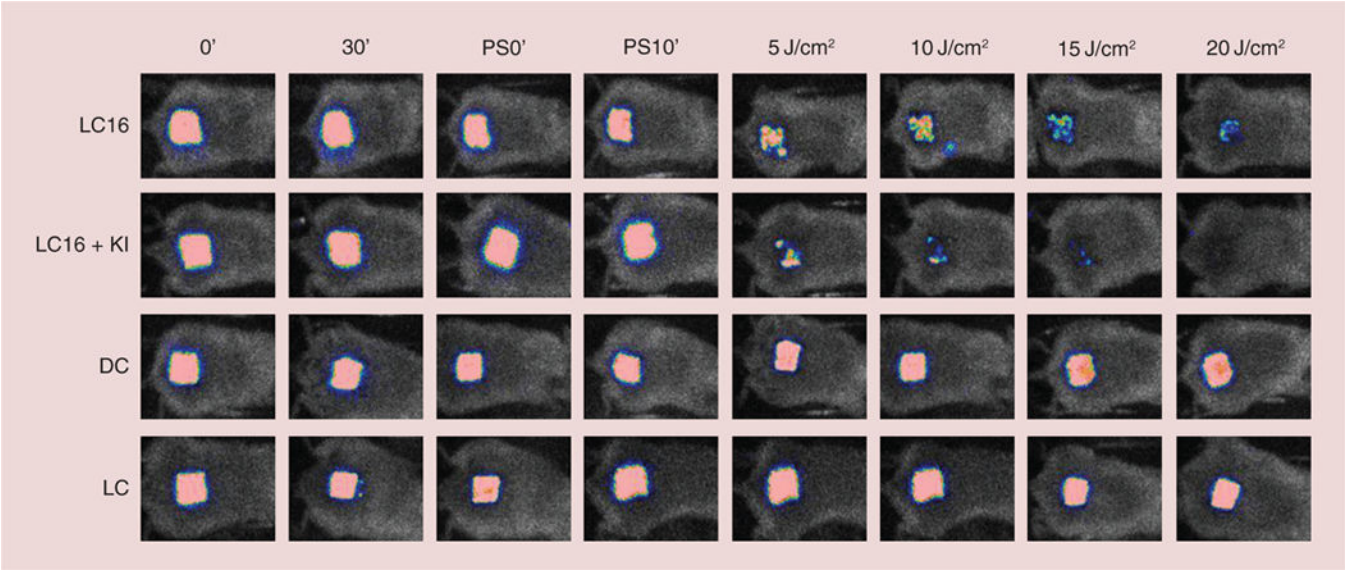

Figure 5. Panel of successive bioluminescence images of representative mice with abrasion wounds infected with bioluminescent *Acinetobacter baumannii* (left for 30 min) and treated by topical application of 200 μM C_{60}-fullerene with or without addition of 10 mM KI solution (left for 10 min)

Mice wounds were exposed to increasing fluences of ultraviolet A (5, 10, 15 and 20 J/cm^2) with imaging taking place after each exposure.

DC: Dark control; LC: Light control; LC16: C_{60}-fullerene; PS: Photosensitizer.

Author Manuscript Author Manuscript Author Manuscript Author Manuscript

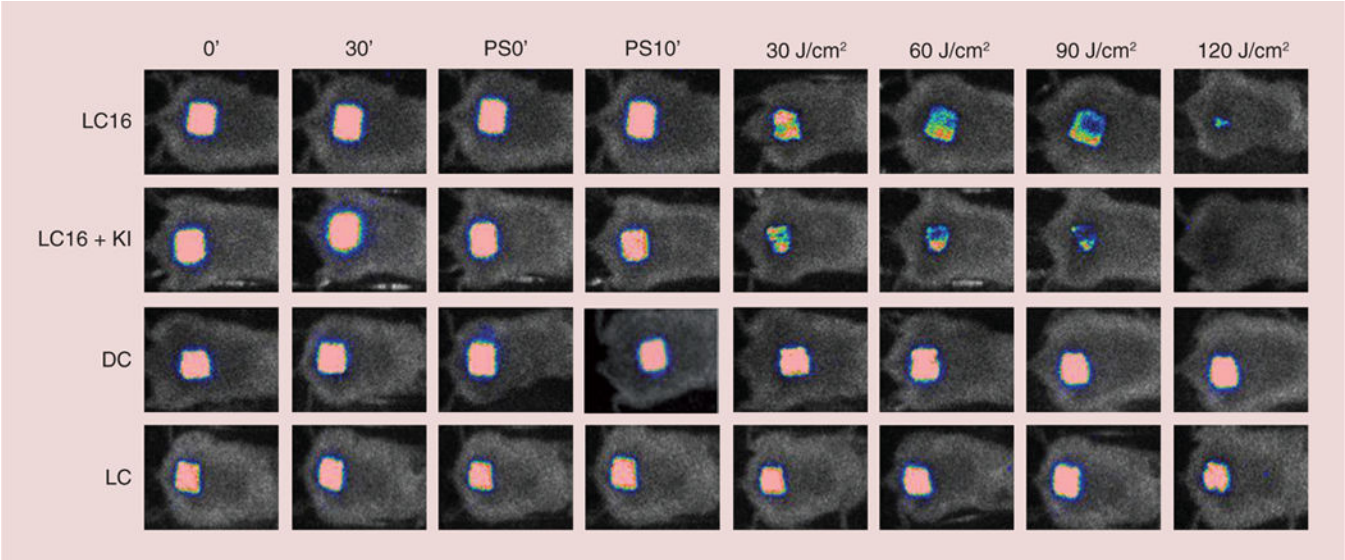

Figure 6. Panel of successive bioluminescence images of representative mice with abrasion wounds infected with bioluminescent *Acinetobacter baumannii* (left for 30 min) and treated by topical application of 200 μM C_{60}-fullerene with or without addition of 10 mM KI solution (left for 10 min)

Mice wounds were exposed to increasing fluences of white light (30, 60, 90 and 120 J/cm^2) with imaging taking place after each exposure.

DC: Dark control; LC: Light control; LC16: C_{60}-fullerene; PS: Photosensitizer.

Author Manuscript Author Manuscript Author Manuscript Author Manuscript

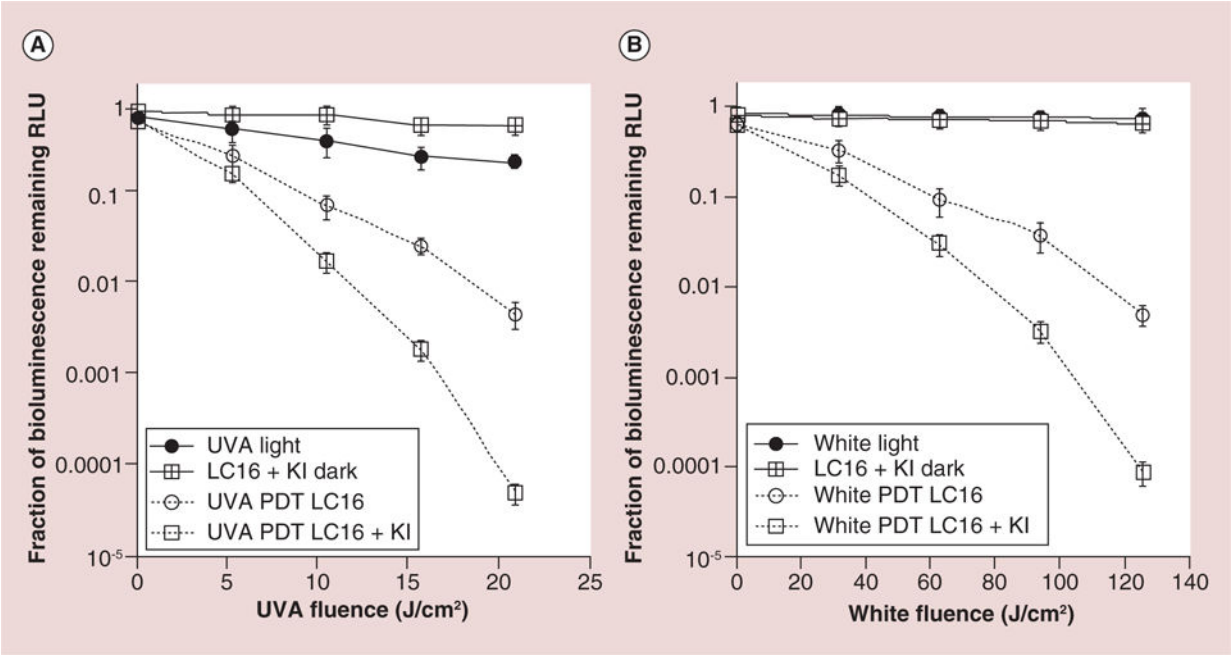

Figure 7. Quantification of relative light units from bioluminescence images captured from groups of mice (n = 6) with *Acinetobacter baumannii* infected wounds treated with C60-fullerene +/− KI and light

(A) UVA light-treated mice shown in Figure 5; **(B)** White light-treated mice shown in Figure 6.

LC16: C_{60}-fullerene; PDT: Photodynamic therapy; RLU: Relative light units; UVA: Ultraviolet A.